Structure and Hyperfine Parameters of E_1' Centers in α-Quartz and in Vitreous SiO_2

Mauro Boero,[1,*] Alfredo Pasquarello,[1,2] Johannes Sarnthein,[1] and Roberto Car[1,2]
[1]*Institut Romand de Recherche Numérique en Physique des Matériaux (IRRMA), IN-Ecublens, CH-1015 Lausanne, Switzerland*
[2]*Département de la Matière Condensée, Université de Genève, 24 Quai E. Ansermet, CH-1211 Geneva, Switzerland*
(Received 10 July 1996)

We report a first-principle study of the E_1' defect in α-quartz and of the analogous E_γ' defect in amorphous SiO_2. Our calculation supports the attribution of both these defects to a positively charged oxygen vacancy. The ground-state configuration of these defects is characterized by a large local relaxation of the atomic network, which leads to a localization of the unpaired electron on a Si dangling bond. Using the calculated electronic spin densities, we fully characterize the hyperfine interactions with nearby ^{29}Si. Our results explain well both the strong and the weak features that are observed in the experimental spectra. [S0031-9007(97)02347-8]

PACS numbers: 61.72.Bb, 71.55.–i, 76.30.Mi

The E_1' center in α-quartz is a prototype defect center observed in various forms of irradiated SiO_2, both crystalline and amorphous. A major motivation for the intensive investigations of this charged defect [1–7] is its responsibility in the degradation of SiO_2-based electronic devices [7,8].

Electron spin resonance (ESR) experiments indicate that the defect is characterized by the presence of an isolated dangling bond of sp^3 character at a silicon site [2]. However, in spite of a considerable theoretical effort to determine its microscopic structure [9–12], a general consensus has not yet been reached.

The most successful model of the E_1' defect in α-quartz is due to Feigl, Fowler, and Yip [11], who associated this center to a positively charged oxygen vacancy: An asymmetric relaxation of its two neighboring silicon atoms leaves a singly occupied dangling bond on one of the two. This model was improved by Rudra and Fowler [12] who suggested that the asymmetric relaxation is stabilized by the formation of a threefold coordinated oxygen atom, giving rise to a puckered configuration. Subsequently, first-principle calculations by Allan and Teter [13] showed that both the configuration proposed by Rudra and Fowler and that corresponding to a silicon dimer bridging the vacancy were metastable. Further semiempirical cluster calculations [14] investigated a possible bistability associated with these two configurations. However, a conclusive picture of the relative stability of the various competing configurations is still missing.

In vitreous SiO_2, the E_γ' defect exhibits very similar ESR characteristics to E_1' [5,6], suggesting that an oxygen vacancy may also be responsible for this defect. The difficulty in modeling a disordered amorphous network has so far prevented realistic calculations to support this conjecture.

In this work, we study the lattice distortions induced in both crystalline and vitreous SiO_2 by an oxygen vacancy in the neutral and in the positive charge state. Our calculations are based on density functional theory within the local spin density approximation. For a-SiO_2 we use a realistic atomic structure generated by quenching from the melt within first-principle molecular dynamics [15]. We first establish the relative stability of the competing metastable structures in α-quartz. We find that both the neutral and the positively charged vacancy constitute bistable defect centers in which the lowest energy configuration changes with the charge state: The silicon dimer configuration is the most stable in the neutral case, whereas the puckered configuration is favored in the positively charged state. In the latter case, we calculate the hyperfine parameters using the electronic wave functions obtained from first principles. The comparison of calculated and experimental [4] hyperfine parameters shows very good agreement. We find that the same bistable behavior also occurs in vitreous SiO_2 when the disordered network allows the stabilization of the puckered configuration by the formation of a threefold coordinated oxygen. Thus our results support the notion that an oxygen vacancy is responsible for both the E_1' defect in α-quartz and for its analog E_γ' in a-SiO_2.

We performed structural relaxations using the Car-Parrinello method [16]. Only valence electrons were explicitly considered, and pseudopotentials (PP's) were used to account for the core-valence interactions. We used a norm-conserving [17] and an ultrasoft PP [18] for silicon and oxygen, respectively. The exchange and correlation energy was included using the formulas in Ref. [19]. A detailed description of the method is given in Ref. [20].

We used a plane-wave basis set with energy cutoffs of 16 and 150 Ry for the wave functions and for the augmented electron density, respectively. This gives good convergence for the electronic ground-state properties [15]. For α-quartz we took a tetragonal supercell ($18.58 \times 16.09 \times 20.43$ atomic units) corresponding to the experimental lattice parameters [21]. For vitreous SiO_2 we used the structure previously generated in Ref. [15], which reproduces very well several

experimental properties of a-SiO_2 [22]. In both the crystalline and the amorphous case, prior to the creation of the defect, our cell contained 24 formula units and the internal structural parameters were fully relaxed. The Brillouin zone of the cell was sampled only at the Γ point.

In α-quartz, each oxygen atom forms a short bond (SB) of 1.610 Å and a long bond (LB) of 1.614 Å to silicon atoms. Although the difference in these bond lengths is negligible, it indicates an asymmetry in the local geometry. From experiments [2], one infers that the silicon atom on the SB side is the site of the unpaired electron. In the following, we will refer to this atom as to Si(0).

We first created a charged vacancy by removing one O atom plus one electron [23]. The system formed a very weak Si-Si bond of 3.05 Å, essentially unchanged with respect to the bulk distance of 3.06 Å. This metastable configuration cannot account for the observations of the E_1' defect, since it does not contain an isolated sp^3-like dangling bond. In our search for other metastable structures we found that the puckered configuration suggested in Ref. [12] is the minimum energy configuration, lower by 0.3 eV than the Si dimer structure. In the puckered configuration the Si(0) atom remains essentially undistorted while the Si atom facing the vacancy on the LB side [Si(1)] undergoes a large distortion in order to bind to a nearby O atom, which then becomes threefold coordinated. The bonds of this atom with its original Si neighbors have lengths of 1.77 and 1.78 Å (cf. to 1.61 Å in the undistorted crystal), whereas the bond length with the Si(1) atom is of 1.82 Å. The resulting configuration of the threefold-coordinated oxygen complex is quasiplanar. In agreement with Ref. [13], we found that the puckering can only occur on the LB side.

In Fig. 1(a), we show the relative energies of the dimer and of the puckered configuration as a function of the Si(0)-Si(1) distance. By calculating the energy of a series of intermediate configurations in which all the degrees of freedom but the Si-Si distance were relaxed, we found that an energy barrier of 0.4 eV has to be overcome to relax from the dimer to the puckered configuration.

When the missing electron is given back to the system to recover a neutral vacancy, the two configurations remain local minima, as shown in Fig. 1(b). However, in this case, the dimer is characterized by a stronger bond with a length of 2.52 Å and is 2.3 eV lower in energy than the puckered configuration. A barrier of 0.3 eV has to be overcome to move from the puckered to the dimer configuration.

We then investigated whether the oxygen vacancy model can explain the E_γ' center in a-SiO_2. The strong similarity between this defect and the E_1' center, in the formation process and in the ESR response, suggests that a similar microscopic model should be at the origin of both defects. Since in vitreous SiO_2 all the sites are nonequivalent, the choice of an adequate vacancy site for the E_γ' center is important. As a rough criterion, we considered the presence of a nearby oxygen atom which could stabilize a puckering distortion. In this way, we could identify a few sites of our amorphous sample as candidates for the E_γ' center. Indeed, by creating a positively charged oxygen vacancy on one of such sites, we found two local minima corresponding to a dimer and to a puckered configuration, as shown in Fig. 1(a). Notice that the puckered configuration is more stable than the dimer one by approximately the same amount of energy as in the crystal, i.e., by $\approx$0.4 eV. The different Si(0)-Si(1) distances in the glass with respect to the crystal reflect the higher flexibility of the amorphous network. The Si dimer is, in this case, extremely weak with a bond length of 3.29 Å, which is larger than the distance between the Si atoms (3.04 Å) prior to the creation of a vacancy. The charge density of the unpaired electron in the dimer configuration is almost equally distributed between the two Si atoms, and therefore this structure cannot account for the ESR observations.

As a second example, we considered a case with no suitable oxygen candidate to stabilize a puckered configuration. In this case, the only locally stable minimum corresponds to a dimer configuration. Clearly, an amorphous sample is characterized by a continuous distribution of different configurations, and a comprehensive study would require a meaningful statistical average. This is beyond the scope of the present investigation.

So far, we have confirmed that a charged oxygen vacancy can give rise to an isolated dangling bond both in crystalline and in amorphous SiO_2. In order to make direct contact with ESR experiments, we calculated the hyperfine parameters. The hyperfine Hamiltonian,

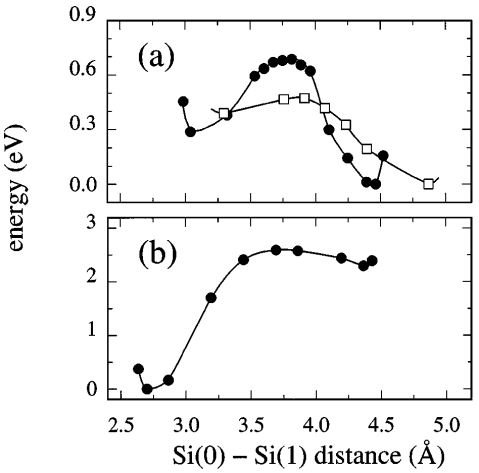

FIG. 1. Total energies of the (a) positively charged oxygen vacancy as a function of the Si(0)-Si(1) distance in α-quartz (circles) and vitreous SiO_2 (squares). The minima at 4.46 and 4.87 Å correspond to puckered configurations. Similarly in (b), for the neutral oxygen vacancy in α-quartz. The lines are guides to the eyes.

$\hat{H} = \vec{S} \cdot \mathbf{A} \cdot \vec{I}$, is given in terms of the hyperfine tensor $\mathbf{A}$ which describes the coupling between the electronic $\vec{S}$ and the nuclear $\vec{I}$ spin at a site $\mathbf{R}$. The components of $\mathbf{A}$ are given by $A_{ij} = a\,\delta_{ij} + b_{ij}$, where

$$a = \frac{8\pi}{3}\, g_e \mu_e g_{\mathrm{Si}} \mu_{\mathrm{Si}} \rho_s(\mathbf{R}), \tag{1}$$

$$b_{ij} = g_e \mu_e g_{\mathrm{Si}} \mu_{\mathrm{Si}} \int d^3 r\, \rho_s(\mathbf{r})\, \frac{3 r_i r_j - \delta_{ij} r^2}{r^5}. \tag{2}$$

In Eqs. (1) and (2), $\rho_s = \rho_\uparrow - \rho_\downarrow$ is the electron spin density, g_e the free-electron g factor, μ_e the Bohr magneton, g_{Si} the nuclear gyromagnetic ratio for Si, μ_{Si} the corresponding nuclear magneton, and the position vector $\mathbf{r}$ is given with respect to the nuclear site $\mathbf{R}$. The isotropic contribution a to the hyperfine tensor corresponds to the Fermi contact interaction, whereas the anisotropic contribution b_{ij} results from dipole-dipole interactions.

The calculation of A_{ij} requires knowledge of the electron spin density in the core region, which is not explicitly provided by our PP calculations. To overcome this difficulty we adopted the scheme recently proposed by Van de Walle and Blöchl [24], who showed that accurate hyperfine parameters can be extracted from a PP calculation by appropriately including all-electron atomic information.

Diagonalization of the A_{ij} matrix provides the eigenvalues and the angles defining the principal directions, which can be compared directly to those extracted from ESR measurements. We first considered the case of α-quartz, for which accurate experimental data are available [2,4]. We oriented the crystal in the same way as in the experiment of Ref. [4]. The hyperfine parameters corresponding to the silicon sites with the strongest hyperfine interaction are reported in Table I.

The strongest feature A_{strong} corresponds to the site of the silicon atom Si(0), where the dangling bond is localized. The axial symmetry of this interaction is well reproduced by the calculation. The agreement for both the eigenvalues and the angles is remarkable. The largest discrepancies between theoretical and experimental angles occur for nonaxial directions, for which the experimental determination is less accurate because of the quasidegeneracy of the corresponding eigenvalues [4].

TABLE I. Hyperfine parameters for α-quartz. Experimental data are from Ref. [4].

	Experiment			Theory		
	Values (MHz)	θ	ϕ	Values (MHz)	θ	ϕ
A_{strong}	1269.7	114.1°	229.7°	1434.5	113.0°	228.3°
	1095.0	128.3°	340.4°	1248.5	101.3°	318.5°
	1094.5	132.1°	115.9°	1245.5	159.0°	70.4°
$A_{1\mathrm{weak}}$	27.5	140.7°	284.5°	61.9	141.6°	281.8°
	22.3	125.5°	133.9°	45.3	127.0°	157.3°
	22.1	104.6°	33.1°	45.9	119.3°	50.3°
$A_{2\mathrm{weak}}$	26.0	58.9°	260.9°	67.3	59.7°	252.9°
	21.0	104.4°	179.9°	51.3	93.3°	168.6°
	20.9	35.0°	111.4°	50.3	25.3°	78.6°
$A_{3\mathrm{weak}}$				11.5	131.4°	347.3°
				10.2	99.6°	186.6°
				9.6	148.7°	83.3°

The weak features, $A_{1\mathrm{weak}}$ and $A_{2\mathrm{weak}}$, are associated with the silicon atoms Si(2) and Si(3) of Fig. 2 [25]. In this case, the agreement between theory and experiment is roughly within a factor of 2 for the eigenvalues but still very good for the angles. This can be explained as follows. The angles depend on a qualitative feature of the charge distribution, namely, its local symmetry, whereas the eigenvalues are determined by the strength of the contact interaction, which depends on the exponential tails of the charge distribution. Quantitative errors in the eigenvalues similar to those found here are typical of the present approach [24]. Thus our calculation indicates that the weak features of the hyperfine spectrum are due to ^{29}Si. This conclusion is in accord with the electron-nuclear double resonance data of Ref. [4].

The atom Si(4) in Fig. 2 gives an additional much weaker hyperfine interaction $A_{3\mathrm{weak}}$. Although this feature was already observed by Silsbee [2], a complete experimental characterization of its hyperfine tensor has not been possible. Since Si(0) has three nearest Si neighbors, one could expect that the three secondary features should have approximately equal strength. This is not the case because, in the presence of a vacancy, Si(4) is not equivalent by symmetry to Si(2) and Si(3) [12]. This effect is apparent in Fig. 3, which shows that the electron spin density at Si(4) is significantly smaller than at Si(2) and Si(3).

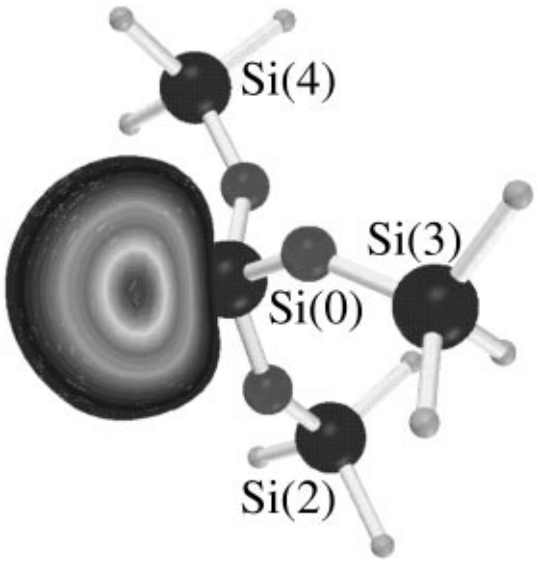

FIG. 2. Ball and stick representation of the site with the unpaired electron. Notation from Ref. [4].

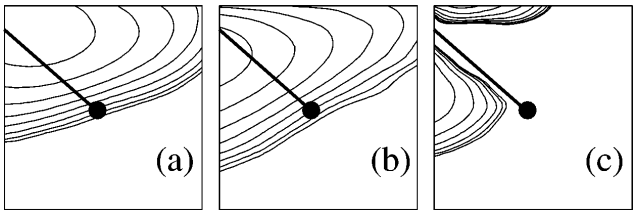

FIG. 3. Electron spin density in each of the three planes containing (a) the Si(0)-O-Si(2), (b) Si(0)-O-Si(3), and (c) Si(0)-O-Si(4) bonds, which connect the silicon atom carrying the dangling bond to its neighbor silicon atoms. The plots focus on regions of 1.2×1.2 Å^2 centered at the latter silicon atoms (indicated as discs). The contour lines correspond to charge densities of $2^n \times 10^{-5}$ atomic units for $n = 0, 1, .., 7$.

We have also calculated the eigenvalues of the hyperfine tensor for the single puckered configuration considered in vitreous SiO_2. Similarly to α-quartz, the largest eigenvalues are associated to the Si atom carrying the unpaired electron. The experimental value for this feature ($A^{\rm exp}_{\rm strong} = 1176$ MHz [5]) compares well with the spherical average of the three largest eigenvalues found in our calculation ($A^{\rm th}_{\rm strong} = 1442$ MHz). The average of the eigenvalues associated to nearest-neighbor Si atoms gives a weak feature, $A^{\rm th}_{\rm weak} = 50$ MHz, which can be compared with the experimental value of $A^{\rm exp}_{\rm weak} = 35$ MHz [6]. However, the attribution of this feature entirely to ^{29}Si is uncertain, and its origin might be due at least partially to protons [6].

In conclusion, we have presented evidence that supports the positively charged oxygen vacancy model as the microscopic origin of both the E_1' center in α-quartz and the E_γ' center in a-SiO_2. This explains the strong similarity between these two defects. Our calculations for α-quartz indicate that the oxygen vacancy constitutes a bistable center, in which the ground state depends on the charge state. The bistability of the neutral vacancy may play a role in the precursor mechanism responsible for the formation of the E_1' center [4].

We acknowledge support of the Swiss National Science Foundation under Grant No. 20-39528.93. The calculations were performed on the NEC-SX3 of the Swiss Center for Scientific Computing (CSCS) in Manno.

*Present address: Max-Planck-Institut für Festkörperforschung, Heisenbergstrasse 1, 70569 Stuttgart, Germany.

[1] R. A. Weeks, J. Appl. Phys. **27**, 1376 (1956); Phys. Rev. **103**, 570 (1963).
[2] R. H. Silsbee, J. Appl. Phys. **32**, 1459 (1961).
[3] G. D. Watkins and J. W. Corbett, Phys. Rev. **134**, A1359 (1964).
[4] M. G. Jani, R. B. Bossoli, and L. E. Halliburton, Phys. Rev. B **27**, 2285 (1983).
[5] D. L. Griscom, Phys. Rev. B **20**, 1823 (1979).
[6] D. L. Griscom, Phys. Rev. B **22**, 4192 (1980).
[7] D. L. Griscom, D. B. Brown, and N. S. Saks, in *The Physics and Chemistry of SiO_2 and Si-SiO_2 Interface*, edited by C. R. Helms and B. E. Deal (Plenum Press, New York, 1988), p. 287, and references therein.
[8] See, for example, E. H. Nicollian and J. R. Brews, *MOS (Metal Oxide Semiconductor) Physics and Technology* (Wiley, New York, 1982).
[9] G. N. Greaves, J. Non-Cryst. Solids **32**, 295 (1979).
[10] G. Lukovsky, Philos. Mag. B **41**, 457 (1980).
[11] F. J. Feigl, W. B. Fowler, and K. L. Yip, Solid State Commun. **14**, 225 (1974).
[12] J. K. Rudra and W. B. Fowler, Phys. Rev. B **35**, 8223 (1987).
[13] D. C. Allan and M. P. Teter, J. Am. Ceram. Soc. **73**, 3247 (1990).
[14] K. C. Snyder and W. B. Fowler, Phys. Rev. B **48**, 13 238 (1993).
[15] J. Sarnthein, A. Pasquarello, and R. Car, Phys. Rev. Lett. **74**, 4682 (1995); Phys. Rev. B **52**, 12 690 (1995).
[16] R. Car and M. Parrinello, Phys. Rev. Lett. **55**, 2471 (1985).
[17] G. B. Bachelet, D. R. Hamann, and M. Schlüter, Phys. Rev. B **26**, 4199 (1982).
[18] D. Vanderbilt, Phys. Rev. B **41**, 7892 (1990).
[19] J. P. Perdew and A. Zunger, Phys. Rev. B **23**, 5048 (1981).
[20] A. Pasquarello *et al.*, Phys. Rev. Lett. **69**, 1982 (1992); K. Laasonen *et al.*, Phys. Rev. B **47**, 10 142 (1993).
[21] J. Glinnemann *et al.*, Z. Krystallogr. **198**, 177 (1992).
[22] In the present work, the structure of Ref. [15] was further relaxed at the experimental density of 2.20 g/cm^3.
[23] The charge neutrality of the simulation cell is ensured by adding a uniform background of negative charge.
[24] C. G. van de Walle and P. E. Blöchl, Phys. Rev. B **47**, 4244 (1993).
[25] The Si atoms are labeled following Ref. [4], where the sites have been crystallographically identified.